2013

Modeling of Particle Agglomeration in Nanofluids

Hari Krishna Kanagala
Lehigh University

Modeling of Particle Agglomeration in Nanofluids

by

Hari Krishna Kanagala

A Thesis

Presented to the Graduate and Research Committee

of Lehigh University

in Candidacy for the Degree of

Master of Science

in

Mechanical Engineering

Lehigh University

(April 2013)

Thesis is accepted and approved in partial fulfillment of the requirements for the Master of Science in Mechanical Engineering

Modeling of Particle Agglomeration in Nanofluids
Hari Krishna Kanagala

……..
Date Approved

……
Dr. Sudhakar Neti
Advisor

……
Dr. Alp Oztekin
Co-Advisor

……
Dr. Gary Harlow
Department Chair Person

Acknowledgement

I would like to express my sincere gratitude to my advisors Prof. Sudhakar Neti and Prof. Alparslan Oztekin for their continuous support and guidance to my research with great patience and motivation. My sincere gratitude to Dr. Satish Mohapatra at Dynalene Inc. for his continuous guidance and motivation, and thank him for letting me use the lab resources at Dynalene every day. I thank Dr. Sreya, George, Lauren, Kevin and Becky for their help with the use of lab and lab equipment at Dynalene. I thank Dr. Pawan for his suggestions to my experimental work and Dr. Srinivas Mettu for his suggestions to my research. I thank Lehigh University librarians for promptly sending me much copyrighted literature to assist with my research.

Lastly, I owe to my parents and sister, and my best friend Priya for their patience, love, and mental support in continuing with my research.

Table of Contents

List of Figures

Abstract

Nanofluids are colloidal dispersions of nano sized particles (<100nm in diameter) in dispersion mediums. They are of great interest in industrial applications as heat transfer fluids owing to their enhanced thermal conductivities. Stability of nanofluids is a major problem hindering their industrial application. Agglomeration and then sedimentation are some reasons, which drastically decrease the shelf life of these nanofluids. Current research addresses the agglomeration effect and how it can affect the shelf life of a nanofluid. The reasons for agglomeration in nanofluids are attributable to the interparticle interactions which are quantified by the various theories. By altering the governing properties like volume fraction, pH and electrolyte concentration different nanofluids with instant agglomeration, slow agglomeration and no agglomeration can be produced. A numerical model is created based on the discretized population balance equations which analyses the particle size distribution at different times. Agglomeration effects have been analyzed for alumina nanoparticles with average particle size of 150nm dispersed in de-ionized water. As the pH was moved towards the isoelectric point of alumina nanofluids, the particle size distribution became broader and moved to bigger sizes rapidly with time. Particle size distributions became broader and moved to bigger sizes more quickly with time with increase in the electrolyte concentration. The two effects together can be used to create different temporal trends in the particle size distributions. Faster agglomeration is attributed to the decrease in the electrostatic double layer repulsion forces which is due to decrease in the induced charge and the double layer thickness around the particle. Bigger particle clusters show lesser agglomeration due to reaching the equilibrium size. The procedures and processes described in this work can be used to generate more stable nanofluids.

Key words: Nanofluids, Colloids, Particle Agglomeration, Interaction Potential Energy, Double Layer, Fortran, Population Balance Equations.

Chapter 1. Introduction

1.1. Colloidal Dispersions

Colloidal dispersion is a homogenous mixture of colloidal particles or colloids with size ranging between 1 nanometer (1nm $=10^{-9}$m) and 1 micrometer (1μm $=10^{-6}$m) in a dispersion medium. A commonly known colloidal dispersion is milk which is an emulsified colloid of fat in the water based medium. The science related to the study of colloidal dispersions is known as Colloid Science which has seen substantial progress since 1860s. Many factors go into preparing a stable colloidal dispersion as solid colloids tend to agglomerate at favorable conditions and get settled due to higher density than medium. Colloids have vast applications in the real world not limited to biology, medicine, agriculture and engineering. One application of solid colloids is in thermal fluids, as it is well known that dispersing solid particles in heat transfer fluids enhanced their thermal properties. Due to big size of these particles many problems like clogging and settling have been visually noticed which created a particular interest on investigation of nanoparticles as colloids.

1.2. Nanofluids

Nanofluids are the colloidal dispersions with nano sized particles known as nanoparticles in the dispersion phase. The sizes of nanoparticles typically range between 1nm to 100nm. Commonly used heat transfer fluids as dispersion medium are Deionized water, ethylene glycol, etc. Advanced technologies have been developed to produce nanoparticle at different sizes and shapes like spherical, rod, planar, etc. Two methods are mainly used to produce nanoparticles viz. 'top down' where bulk materials are milled, and 'bottom up' where chemical processes are used to evolve the nanoparticles from atoms and molecules. Generally, a distribution is observed in particle sizes when nanoparticles are produced, with maximum number of particles possessing average

particle size. Park et al. (2005) observed that the thickness of the size distribution can be controlled by controlling the aggregation of particles during production. Owing to their small size and relatively large surface area nanoparticles dispersed in the nanofluids have created considerable interest in recent times for their improved heat transfer properties. Pioneering researchers at Argonne National Laboratory started experimenting with nanofluids to increase the thermal conductivity (Choi (1995), Eastman et al. (2001), Lee et al. (1999)), and have reported anomalous enhancement in the thermal conductivity of nanofluids. Even with nanoparticles many of the nanofluids are found unstable with settling being visually observed in the dispersions which is attributed to the coagulation or agglomeration of the nanoparticles.

1.3. Particle Agglomeration

In chemical terms, agglomeration is a process in which colloidal particles mutually interact due to Brownian motion, which is described as a random motion of particles in the dispersed medium due to collision with atoms or molecules of the medium, and combine with adjacent ones to form clusters of small particles. The word agglomeration is synonymous with flocculation, aggregation and coagulation. During agglomeration particles in clusters experience a net attractive force which depending on the conditions requires great amount of energy to bring them apart. This attractive force is known as van der Waals force, which at molecular level is resulted due to the interaction between dipoles on molecules. According to London theory, the interaction energy $V_{int}(R)$ (Equation 1) depends on the inverse sixth power of the separation between molecules, where R is the separation between molecules.

$$V_{int}(R) \;\; \alpha \;\; {}^{1}/_{R^6} \qquad \ldots\ldots\ldots\ldots\ldots\ldots\ldots\ldots\ldots (1)$$

Summation of all the intermolecular interaction energies between the colloidal particles gives the long-range van der Waals interaction energy between colloids which usually is

negative implying the attractive forces. If there are no other interparticle forces, then the particles get mutually attracted resulting in clusters formation. Due to increase in the size of clusters with agglomeration, dispersed particles get settled with gravity. Agglomeration can be controlled or altered by changing surface properties of the colloidal particles by inducing surface charges and by forming polymer layer around the particles which generate repulsive forces between the particles and keep them apart from forming clusters. Unless charged, the nanoparticles obtained from the manufacturer are in agglomerated form due to predominant attractive forces between them. Ultrasonication is a method of agitating the liquid sample, nanofluid in particular, by irradiating the sample with ultra-sonic sound waves (>20 kHz frequency). While preparing nanofluids by adding particles into base fluid, large amount of energy is supplied by ultrasonication to break the agglomerates in to individual nanoparticles in nanofluid. Particle agglomeration is studied in detail in the current research.

1.4. Literature Survey

Resource full of research has been carried out to study factors effecting agglomeration and effects of agglomeration on rheological and heat transfer characteristics of nanofluids.

Islam et al. (1995) presented a review on heteroaggregation, which is the interaction between the particles with different sizes, shapes, surface charge, etc. in dispersion medium. They have presented the modified expressions for interaction energies and stability ratio by including the heteroaggregation effects. Experimental studies performed by many researches have been presented to validate the heteroaggregation phenomenon.

Das et al. (2003) investigated heat transfer characteristics of alumina/water nanofluids at different concentrations between 4 to 16 percent by weight. They prepared

nanofluids without inducing any electrostatic repulsion between particles and without any stabilizers like surfactants. By ultrasonicating the nanofluid they observed the nanofluids remain stable for about 6 hours. The nanoparticles were found to sediment on the heater and deteriorating the boiling performance. With increase in concentration the sedimentation was increased implying the increase in the agglomeration with concentration.

Lo & Tsung (2005) observed that agglomeration in CuO nanofluid was changing with time and changes in the ambient temperature. At subzero temperatures the average particle size of the nanofluid changed very rapidly to large sizes, but no consistent trend in the increase of average particle size was observed with increase in the temperature although there was an increase in the average particle size with time.

Lee et al. (2006) studied influence of the surface charge on particle aggregation in nanofluids. They have regulated the particle surface charge with pH and observed increase in the surface charge with decrease in pH from the isoelectric point due to increase in the concentration of potential-determining ions (H^+ and OH^-). With increase in the surface charge or decrease in the pH they have observed increase in the stability of the nanofluid which is attributed to the increase in the electrostatic repulsive energy between the nanoparticles. Also the thermal conductivity increased with change in the pH away from the isoelectric point, and with increase in the volume fraction.

Timofeeva et al. (2007) observed the effect of agglomeration of particles on thermal conductivity of alumina nanofluids. With 11nm particles they observed larger agglomerates than with 40nm particles, and the size of the agglomerated particles increased with time. The thermal conductivity of the nanofluid depended on the shape the particles with elliptical nanoparticles showing greater enhancement.

Lee et al. (2008) has prepared alumina nanofluids from 0.01 percent to 0.3 percent concentrations without adding any surfactants and ultrasonicating up to 20 hours. They have observed higher zeta potential in ultrasonicated nanofluid to the one which was not sonicated, and the zeta potential increased with increase in the duration of ultrasonication, before attaining a constant value. Nanofluids ultrasonicated above 5 hours are found dispersed with very little agglomeration. The viscosity and thermal conductivity enhanced with increase in volume fraction of the nanoparticles dispersed.

Yang et al. (2012) studied the effect of agglomeration on thermal conductivity and viscosity of the nanofluids. Wide range of nanofluids has been prepared with different base fluids and different nanoparticles at various volume fractions, and with and without adding any stabilizers. It has been observed that agglomeration was increasing with time which is evident from increase in average particle size of the nanofluids. It was also observed that agglomeration in nanofluids has negligible effect on the thermal conductivity, although both thermal conductivity and viscosity increased with increase in the volume fraction of nanofluids.

1.5. Aim and objective

From the literature survey it is noticed that there has been a considerable enhancement in heat transfer characteristics with nanofluids. Agglomeration of nanoparticles is increasing with time and has a strong effect on rheology and heat transfer characteristics of nanofluids. It is evident that more than rheology and heat transfer characteristics it is the stability of the nanofluid that strongly decides the usage of nanofluid as a heat transfer fluid. Many researchers have quantitatively addressed the reasons for aggregation between two similar or different particles in a dispersion medium and attributed them to surface chemistry of the particles. It is important to analyze the agglomeration of all the particles in the nanofluid, and how the particle size distribution is effected with time.

Present research is aimed at quantitatively addressing the agglomeration in nanofluids with time, taking into consideration the interactions of large number nanoparticles of different sizes along with the effects of dispersion medium. A numerical model has been created in Fortran 2003 language which solves the population balance equations with different rates of agglomeration. From the particle size distributions obtained as output from the model, the effect of various parameter on the rate of agglomeration in nanofluids is studied.

Chapter 2. Mathematical Model

2.1. Population Balance Equations

Population Balance Equations (PBEs) have diverse applications in areas involving particulate systems like crystallization, aerosol dynamics, colloidal aggregation, etc. These are integro-partial differential equations with the general form for pure aggregation is given as (Equation 2) where $n(v,t)$ is the number density of particles per unit volume of fluid.

$$\frac{\partial n(v,t)}{\partial t} = \frac{1}{2}\int_0^v \beta(v-v',v')n(v-v',t)\,n(v',t)dv' - n(v,t)\int_0^\infty \beta(v,v')n(v',t)dv' \ldots\ldots\ldots\ldots (2)$$

The first term on right hand side corresponds to the birth rate of the particulate clusters of size v due to collision of smaller particles with sizes v-v' and v', and the second term corresponds to the death rate of the particles due to collisions with other particles to form particulate clusters of size v particular size. And integrating both the effects gives the rate of change of number density of particles of size v. Other phenomena like nucleation and growth of particles can be conveniently included into the population balance equations by adding corresponding effect terms on right hand side of the Equation 2. The kinetics of the agglomeration is attributed to the rate kernels $\beta(v\text{-}v',v')$ and $\beta(v,v')$ inside the Birth and Death rate terms.

2.1.1. Discretized PBEs

To solve Population Balance Equations, several numerical techniques like method of moments, method of weighted residuals or method of discretization are available. Method of discretization is considered in the present research owing to its ease in computation. Kumar & Ramkrishna (1996) have proposed a method of discretization in which the particles are distributed into different interval depending on the size.

A particle size grid (Figure 1) is considered with M intervals in such a way that all the sizes of particles in the nanofluids can be accommodated. v_1 corresponds to the size of smallest particle and v_{M+1} corresponds to the size of largest particle in nanofluid. Representative size (x_i) has been assigned to all the particles in a particular interval and related to the end volumes of each interval as $v_i = (x_i + x_{i+1})/2$. The grid can be uniform or

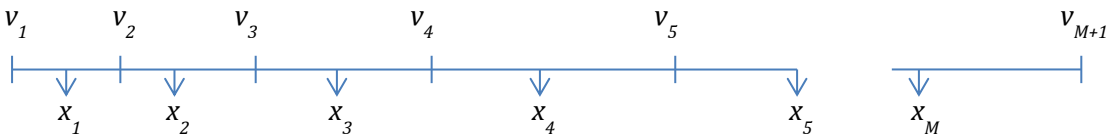

Figure 1 Particle size grid with M intervals

geometric type ($x_{i+1} = rx_i$) with varying coarseness. At a given time, the total number of particles in an interval is represented by $N_i(t)$ which is obtained from the number density distribution in Equation 3.

$$N_i(t) = \int_{v_i}^{v_{i+1}} n(v,t)dv \qquad \ldots\ldots\ldots\ldots\ldots\ldots\ldots\ldots (3)$$

After performing a few mathematical calculations, the discretized population balance equation which is an ordinary differential equation (ODE) is obtained from Equation2 and Equation 3 as (Equation 4).

$$\frac{dN_i(t)}{dt} = \sum_{v_i \le x_j + x_k \le v_{i+1}}^{j \ge k} \left(1 - \frac{\delta_{jk}}{2}\right) \beta_{jk} N_j(t) N_k(t) - N_i(t) \sum_{k=1}^{M} \beta_{ik} N_k(t) \qquad \ldots\ldots\ldots\ldots\ldots\ldots\ldots\ldots (4)$$

The first term on right hand side of Equation 4 is discretized birth rate and the second term is discretized death rate for particles in i^{th} interval. The birth term is considered when the sum of sizes of colliding particles lies between closed interval [v_i, v_{i+1}]. Here, δ_{ij} is the kronecker delta whose value is assigned as '1' if $j=k$ and '0' if $j \neq k$ to

ensure all the particles are counted only once. For every particle size distribution there will be M system of coupled ODEs at each time interval which have to be solved to obtain the number of particles in each size interval. To conserve the first and second moments, Kumar & Ramkrishna (1996) have proposed Equation 5 which can be solved along with Equation 4.

$$\frac{dx_i(t)}{dt} = \frac{1}{N_i(t)} \sum_{v_i \le x_j + x_k \le v_{i+1}}^{j \ge k} \left(1 - \frac{\delta_{jk}}{2}\right) \beta_{jk} \left(x_j + x_k - x_i\right) N_j(t) N_k(t) \qquad \ldots\ldots\ldots\ldots (5)$$

In a particular interval of the grid (Figure 1), if the number density of particles is more towards an end of the interval, then Equation 5 adjusts the representative size of each interval such that the total volume of the particles is preserved accurately.

2.2. Numerical Model

In order to solve the system of population balance equations generated (Equations 4 and 5) a numerical model has been created in Fortran 2003, as presented in Appendix A. To get more accurate distributions, the size of the grid *M* and geometric type width of the intervals are varied depending on the broadness of the particle size distribution from 40 to 60 and from 1.3 to 1.5 respectively. To simplify the discretized population balance equations (Equations 4 and 5) the number of particles in each interval is non-dimensionalized by initial number of particles N_o per unit volume of dispersed medium, and the size of particles is non-dimensionalized by initial average size of particles V_o per unit volume of dispersed medium (Equations 6 and 7).

$$\frac{dN^*_i(t)}{dt^*} = (N_o t_o) \left\{ \sum_{v^*_i \le x^*_j + x^*_k \le v^*_{i+1}}^{j \ge k} \left(1 - \frac{\delta_{jk}}{2}\right) \beta_{jk} N^*_j(t) N^*_k(t) - N^*_i(t) \sum_{k=1}^{M} \beta_{ik} N^*_k(t) \right\} \qquad \ldots\ldots\ldots\ldots (6)$$

$$\frac{dx^*_i(t)}{dt^*} = (N_o t_o) \frac{1}{N^*_i(t)} \sum_{v^*_i \le x^*_j + x^*_k \le v^*_{i+1}}^{j \ge k} \left(1 - \frac{\delta_{jk}}{2}\right) \beta_{jk} \left(x^*_j + x^*_k - x^*_i\right) N^*_j(t) N^*_k(t) \qquad \ldots\ldots\ldots (7)$$

In Equations 6 and 7, N^*, x^*, v^*, t^* are the non-dimensionalized number of particles, representative volume, particle volume and numerical time constant. The rate kernel can be varied depending on the type of reaction under consideration. It has to be observed that at any given time, the total number of particles per unit volume of fluid multiplied by the average size of particles, N_oV_o is for the initial condition, is the volume fraction of nanofluid considered. To validate the numerical model, numerical results obtained for a given constant rate are compared with the analytical solution derived by Scott (1967).

$$n(v,0) = \left(\frac{N_o}{V_o}\right)\left(\frac{4v}{V_o}\right)e^{\left(-\frac{2v}{V_o}\right)} \quad \ldots\ldots\ldots\ldots (8)$$

$$n(v,t) = \left(\frac{N_o}{V_o}\right)\frac{8e^{\left(-\frac{2v}{V_o}\right)}\sinh\left\{2\left(\frac{v}{V_o}\right)\left(\frac{T}{(T+2)^2}\right)\right\}}{T^{\frac{1}{2}}(T+2)^{\frac{3}{2}}};\ T = \beta N_o t \quad \ldots\ldots\ldots\ldots\ldots (9)$$

By considering the initial particle number density distribution as Gaussian-like distribution (Equation 8), the number density of particles at different times is obtained in Equation 9. By assuming the initial average volume of particles as the size of particles with radius 100nm, and constant rate of process as $8k_BT/3\eta$, where k_B is the Boltzmann constant, T is the absolute temperature of particle medium and η is the viscosity of particle medium, the particle distribution is compared between model solution and analytical solution at volume fractions 1 percent (Figure 2) and 0.1 percent (Figure 3). From Figure 2 and 3, the cumulative distribution of number of particles in different intervals at different times is nearly identical for both model solution and analytical solution, thus validating the numerical model.

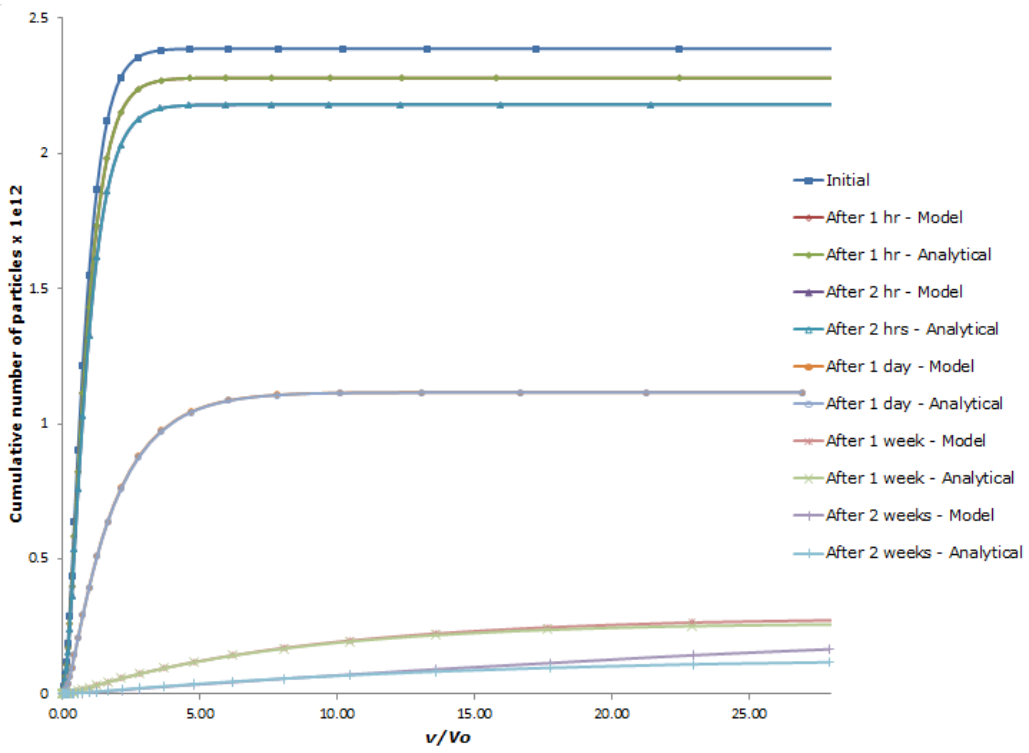

Figure 2 Cumulative particle number distributions for initial Gaussian-like distribution at 1% volume fraction

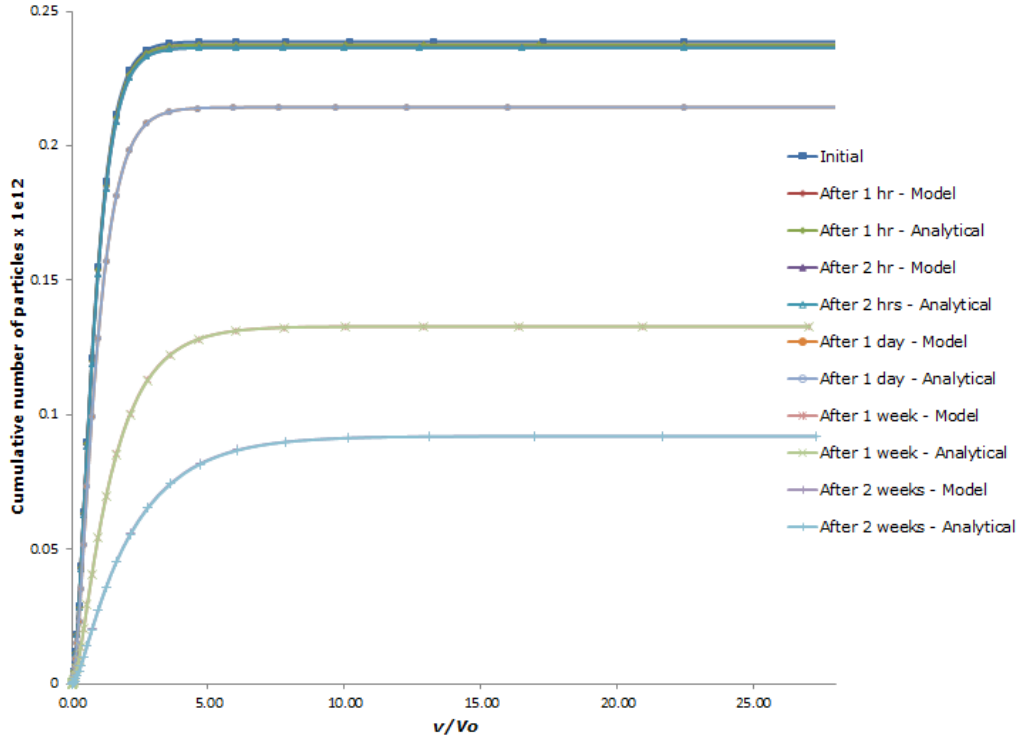

Figure 3 Cumulative particle number distributions for initial Gaussian-like distribution with 0.1% volume fraction

2.3. Rate of Particle Agglomeration

The rate kernel for agglomeration β that appears in Equations 2, 3, 4 and 5 depends on many factors driving the effect. Smoluchowski in 1917 has derived an expression for the collision frequency of particles based on Brownian motion, and obtained the Brownian rate β_b of the collision between two particles with sizes u, v and radii a_1, a_2 as

$$\beta_b = 4\pi(D_1 + D_2)(a_1 + a_2) \quad \ldots\ldots\ldots\ldots\ldots\ldots\ldots (10)$$

$$D_1 = \frac{k_B T}{6\pi\eta a_1} \; ; \; D_2 = \frac{k_B T}{6\pi\eta a_2} \quad \ldots\ldots\ldots\ldots\ldots\ldots\ldots (11)$$

$$\beta_b = \frac{2k_B T}{3\eta}\left(u^{-\frac{1}{3}} + v^{-\frac{1}{3}}\right)\left(u^{\frac{1}{3}} + v^{\frac{1}{3}}\right) \quad \ldots\ldots\ldots\ldots\ldots\ldots\ldots (12)$$

In Equation 10, the diffusion coefficients of particles D_1 and D_2 are obtained from the Stokes-Einstein equation (Equation 11), where k_B is the Boltzmann constant, T is the absolute temperature of particle medium and η is the viscosity of particle medium. Combining both Equations 10 and 11 we get the Brownian rate of two particles with sizes u and v in Equation 12. Equation 12 indicates that the Brownian rate for agglomeration decreases with increase in the particle sizes, increases with decrease in the viscosity of dispersion medium, and increases with increase in temperature of the nanofluid. Not all collisions between particles will lead to the permanent cluster formation. According to the stability theory developed by Deryaguin, Landau, Verwey, and Overbeek, famously referred as DLVO theory, two particles aggregate after collision when the net interaction energy in bringing the two particles to collide is attractive (positive). Total interaction energy V_T is the summation of repulsive energy V_R due to electrostatic double layer repulsive forces around the particles, and attractive energy V_A due to van der Waals attractive forces between the particles. There are also other energies which are not discussed by DLVO theory like stern potential energy due to

addition of polymers and hydration energy due to hydrophobic nature of the particles in aqueous medium. Since the present study considers alumina nanoparticles in aqueous electrolyte medium, only the electrostatic double layer repulsions and the van der Waal attractions have been included in this section.

2.3.1. Van der Waals Attraction Energy

Van der Waals forces between particles are the resultant of summation of all the intermolecular forces between the particles due to interaction of dipoles on molecules. These are attractive in nature, and the interaction energy V_A in bringing the spherical particles of radii a_1, a_2 to a center-center distance R is given by Hamaker (1937) as

$$V_A = -\frac{A_H}{6}\left\{\frac{2a_1a_2}{R^2-(a_1+a_2)^2}+\frac{2a_1a_2}{R^2-(a_1-a_2)^2}+ln\left(\frac{R^2-(a_1+a_2)^2}{R^2-(a_1-a_2)^2}\right)\right\} \quad \ldots\ldots\ldots\ldots(13)$$

Here A_H is the effective Hamaker constant for particles in medium which is observed to be positive for particles with identical material properties.

2.3.2. Electrostatic Double Layer Repulsion Energy

The electrostatic double layer is a layer of dispersion of electrolyte ions around the nanoparticles with a net surface charge. Surface charge can be induced on the nanoparticles by addition of the potential determining ions (*p.d.i*). For the oxide particles like Al_2O_3, CuO etc. in aqueous medium the *p.d.i* are hydrogen and hydroxyl ions whose quantity can be altered by adding acids like HCl, HNO_3 and bases like NaOH, KOH respectively. These particles with a surface charge are surrounded by the oppositely charged ions, called counter-ions, which form a double layer of charges. From the Debye-Hückle theory of electrolytes, the thickness of the electrostatic double layer is expressed as κ^{-1} (in meter)

$$\kappa^{-1} = \sqrt{\frac{\epsilon_o \epsilon_r k_B T}{2 N_A e^2 I}} \quad \ldots\ldots\ldots\ldots\ldots\ldots\ldots\ldots (14)$$

In Equation 14, ε_o is the permittivity of free space, ε_r is the relative permittivity of medium, N_A is the Avogadro number, e is the elementary charge, k_B is the Boltzmann constant, T is the temperature of the medium, and I is sum of the concentration of all ions including the electrolyte ions other than the potential determining ions in the nanofluid. According to the theory, with increase in the electrolyte concentration I (in mol/m^3) the Debye length decreases which in turn decreases stability of the nanofluid. Many researchers have come up with expressions for electrostatic double layer interaction energy with limitations on κH where H is the distance between surfaces of the spheres, but Sader et al. (1995) could obtain a simple expression for electrostatic double layer interaction energy (V_R) as

$$V_R = \epsilon_o \epsilon_r \left(\frac{a_1 a_2}{R}\right)\left[\left(\psi_1 + \psi_2\right)^2 \ln\left(1 + e^{-\kappa H}\right) + \left(\psi_1 - \psi_2\right)^2 \ln\left(1 - e^{-\kappa H}\right)\right] \quad \ldots\ldots\ldots\ldots\ldots (15)$$

Ψ_1 and Ψ_2 in Equation 15 are the potentials on charged nanoparticles and are dependent on the surface charge density of the particles. Here a_1, a_2 are the radius of particles and R is the center-to-center distance between the interacting particles. Equation 15 is accurate for all κH, and is considered as a modified version of Hogg, Healy and Fuerstenau (HHF) expression. From the Debye-Hückle approximation theory expressions for all the potential energies are accurate only for $\kappa a >> 1$ where a is the radius of nanoparticle.

2.3.3. Stability Ratio

The collision efficiency in a Brownian motion is dependent on effectiveness of the potential barrier between the particles keeping them away from forming clusters. This collision efficiency is quantitatively calculated as the stability ratio, W, which is ratio of

the number of collisions between particles to the number of collisions that could result in coagulation between them. In other words, from Hunter & White (1987) the stability ratio, *W*, is ratio of the rate of fast aggregation (R_f) to the rate of slow aggregation (R_s) for a particular nanofluid (Equation 16).

$$W = \frac{R_f}{R_s} = 2\int_2^{\infty} \frac{\exp\left(\frac{V_T}{k_B T}\right)}{s^2} ds\,; \quad s = \frac{2R}{a_1 + a_2} \qquad \ldots\ldots\ldots\ldots\ldots\ldots\ldots (16)$$

In Equation 16, V_T is the total interparticle interaction energy which is summation of the attraction and repulsion energies.

$$V_T = V_A + V_R \qquad \ldots\ldots\ldots\ldots\ldots\ldots\ldots (17)$$

The rate kernel of agglomeration β is then obtained by including the Brownian motion and the collision efficiency from Equations 12 and 16 and is written as

$$\beta = \frac{1}{W}\beta_b = \frac{1}{2\int_2^{\infty} \frac{\exp\left(\frac{V_T}{k_B T}\right)}{s^2} ds} \left[\frac{2k_B T}{3\eta}\left(u^{-\frac{1}{3}} + v^{-\frac{1}{3}}\right)\left(u^{\frac{1}{3}} + v^{\frac{1}{3}}\right)\right] \qquad \ldots\ldots\ldots\ldots\ldots\ldots (18)$$

By substituting the rate kernel for agglomeration in nanofluids (Equation 18) in Equations 6 and 7 and adjusting the grid size and width of the particle size intervals in the numerical model, the particle size distribution at different times can be obtained from the numerical model with a given initial particle size distribution.

Chapter 3. Experimental Investigation

3.1. Preparation of Nanofluids

The present experimental study has been performed using nanofluids consisting of alumina nanoparticles in de-ionized water. Alpha alumina nanoparticles were purchased from Inframat Advanced Materials, USA. According to the manufacturer specifications, the alumina nanoparticles purchased are spherical in shape and polydispersed in terms of their sizes with the particles having an average particle diameter of about 150nm. The density of the nanoparticles is assumed to be 3.97gm/cc, true density of the bulk alumina. The true density is used to calculate the volume of nanoparticles from their weight measured on a sensitive weigh balance, and calculated the volume fraction of the nanofluid by mixing in a particular volume of base fluid. The alumina nanoparticles are not functionalized in anyway and thus since there are no repulsive forces between the alumina nanoparticles in the powder form, the nano powder is observed to have big clusters formed by the aggregation of nanoparticles. Energy is required to break the nanoparticle clusters apart in the de-ionized water, and the energy is supplied to the nanofluids by suspending samples in the VWR 50HT water bath ultrasonicator. It has been observed that about 5-16 hours of continuous ultrasonication is required to break all the particles apart but the energy density (J/Kg) requirements for this de-agglomeration are not apparent. Hydrochloric acid is added to the base fluid until desired pH is reached as quantified with a pH meter. Additionally very small concentrations of sodium chloride electrolyte, often in the order of milli moles of electrolyte per liter of nanofluid, are added to create a layer of counter-ions around each particle to prevent the particles coming closer. To obtain NaCl electrolyte solution at very small concentrations, either a few milligrams of sodium chloride salt is added in neutral de-ionized water, or sodium hydroxide is mixed with hydrochloric acid at required pH until the solution reached neutral value (pH = 7). Different nanofluids are

prepared here with combination of the properties viz. volume fractions 0.05 percent and 0.01 percent, pH values of 3, 3.3 and 4, and electrolyte concentrations 10^{-3}M and 10^{-4}M.

3.2. Particle Size Distribution

Particle size distributions (PSDs) of nanofluids in this study are analyzed using Dynamic Light Scattering (DLS) technique. Other light scattering methods to analyze the PSDs are Rayleigh scattering, Rayleigh-Gans-Debye scattering, and Mie scattering. DLS technique, also known as quasi-elastic light scattering (QELS) or photon correlation spectroscopy (PCS), measures the intensity of the light scattered by the particles incident by the light waves from source. The incident light waves with their high oscillating electric field polarizes the electrons in the particles which in turn generates new oscillating field scattered in all directions as light waves. The interference of the scattered light from all the particles on photomultiplier detector (PMT) is correlated to the diffusion coefficient of particles. From the Stokes-Einstein equation for spherical particles (Equation 11) the diffusion coefficient is used to calculate the radius of the particles.

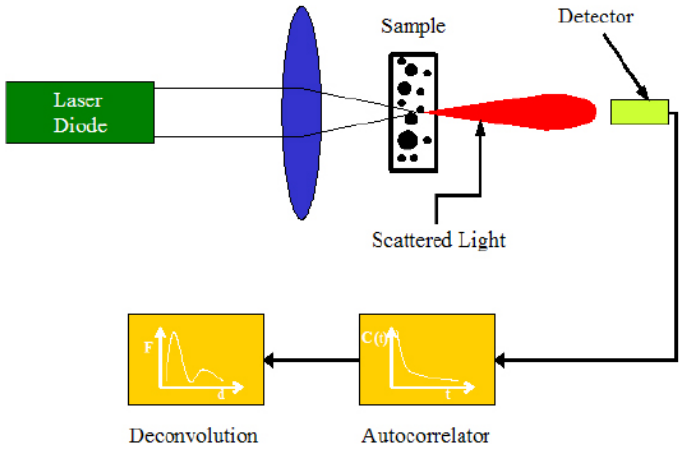

Figure 4 Principle block diagram of the NICOMP 380 Submicron Particle Sizer

NICOMP 380 Submicron Particle Sizer at Dynalene Inc. is used here to analyze the PSDs. Figure 4 illustrates the principle of the NICOMP 380, which uses 5mW HeNe laser at a wavelength of 632.8nm. For each sample analyzed with this instrument the output consists of 6 distributions viz. Intensity weighted, volume weighted and number weighted for both Gaussian and NICOMP distributions. Number weighted distribution considers the particle number density distribution at different particle diameters, and the intensity weighted and volume weighted distributions are obtained by multiplying the number weighted distribution with factors v and v^2 respectively, where v is volume of the particles.

Understanding the changes in the number of particles of a particular size is important to understand the agglomeration phenomenon. Number weighted distribution is more suitable compared to volume weighted distribution to analyze the distribution of particles in the nanofluid and hence number weighted distribution is considered in the further study. Among the Gaussian and NICOMP distributions, Gaussian distribution gives a better fit to the PSD data if the chi squared value reamins small (i.e. below 2 or 3) over the duration of every analysis. The DLS Module makes this judgment automatically and provides an appropriate warning message if the value of chi squared exceeds 3, suggesting that the Gaussian distribution is inappropriate and the NICOMP distribution has to be considered as the final PSD.

3.3. Experimental Procedure

A nanofluid with a particular volume fraction of particles, pH and electrolyte concentration is prepared by adding the required weight of nanoparticles in the base fluid with specific electrolyte concentration and the pH regulated using hydrochloric acid (HCl) and sodium hydroxide (NaOH) in de-ionized water having. During ultrasonication, as pH of the nanofluid is observed to increase due to increase in the surface charge on the nanoparticles, pH is measured at certain intervals during ultrasonication and acid is

added until the pH reached the starting value. After ultrasonicating the nanofluid for sufficiently long time (around 15-16 hours in this study) small quantity of the sample is taken and analyzed immediately using the NICOIMP 380 to yield the initial particle distribution. To get a nearly accurate particle size distribution, the sample which is analyzed on NICOMP should be made sufficiently dilute such that the scattered intensity received by PMT detector is between 250 kHz to 350 kHz. This is accomplished by filling the test cuvette with base fluid at specific pH and electrolyte concentration, and carefully mixing a few drops of nanofluid such that the intensity displayed by NICOMP is between 250 kHz to 350 kHz. Diluting the nanofluid in test cuvettes decreases its volume fraction. Decreasing the volume fraction of nanofluid does not alter the potential energies and the aggregation rate kernel (Equations 13, 15 and 18), but decreases the number of particles in each size interval thus decreasing the rate of change of number of particles of different size intervals at particular time (Equation 4). Since the nanofluid is diluted 50 folds in test cuvettes, it can be conveniently assumed that for the duration of analysis on NICOMP the particle size distribution remains constant due to negligible rate of change of number of particles of different sizes (Equation 4).

Before starting to use the NICOMP to analyze the PSDs of samples, it was checked to meet the instrument manufacturer's specifications. This was accomplished by analyzing a fresh sample of the standard polystyrene latex dispersion for the PSD with standard deviation less than 15 percent, chi squared parameter of less than 3, and base adjustment parameter within 0.05 percent.

The particle size distributions were observed at different time intervals after mixing the nanofluid uniformly each time immediately before measurement. NICOMP recommends the use of Gaussian distribution instead if the chi squared parameter value is less than 3. Taking this into account, after the completion of each analysis on

NICOMP, the values of average particle size and standard deviation for both the volume weighted and the number weighted distributions were recorded.

Chapter 4. Results and Discussions

Just after ultrasonication (time, t = 0 sec), each nanofluid was analyzed for the initial particle size distribution. Figure 5 shows the initial PSDs for several nanofluids. Since the Chi Squared parameter is below three for these distributions, Gaussian distributions are used to analyze the PSDs. Since NICOMP system generates the distributions which are relative to the peak value and on a logarithmic scale, for a better appreciation of the particle size distribution, the data is plotted using a linear abscissa for the measured average particle sizes and standard deviations of (Figure 6). All the nanofluids have initial average particle sizes around 150 nm thus agreeing with the manufacturer's specifications. As the number of particles per unit volume of nanofluid is equivalent to the area under number density distribution, it is observed (Figure 6) that at 0.05 percent volume fraction the nanofluid with $pH = 4$ and $C = 10^{-4}$M NaCl has more number of particles and the nanofluid with $pH = 3.3$ and $C = 10^{-3}$M NaCl has less number of particles.

The PSDs for different nanofluids have been measured and analyzed as a function of time. Figure 7 shows the PSDs of alumina nanofluid at $pH = 3$ and $C = 10^{-4}$M NaCl for 3 weeks duration obtained from both experiments and model. In the similar way Figure 8, Figure 9 and Figure 10 show the PSDs of alumina nanofluids at $pH = 3.3$ and $C = 10^{-3}$M NaCl, and $pH = 4$ and $C = 10^{-3}$M NaCl respectively. From Figure 7 to 10, it is observed that the PSDs of all nanofluids became broader indicating agglomeration with time.

In a nanofluid, the extent of agglomeration is dependent on the brownian rate along with the total interparticle interaction energy (as discusses in Section 2.3). To increase or decrease the stability/shelf life of a nanofluid, the interaction energies between the particles can be controlled within limits by varying the pH and electrolyte concentration.

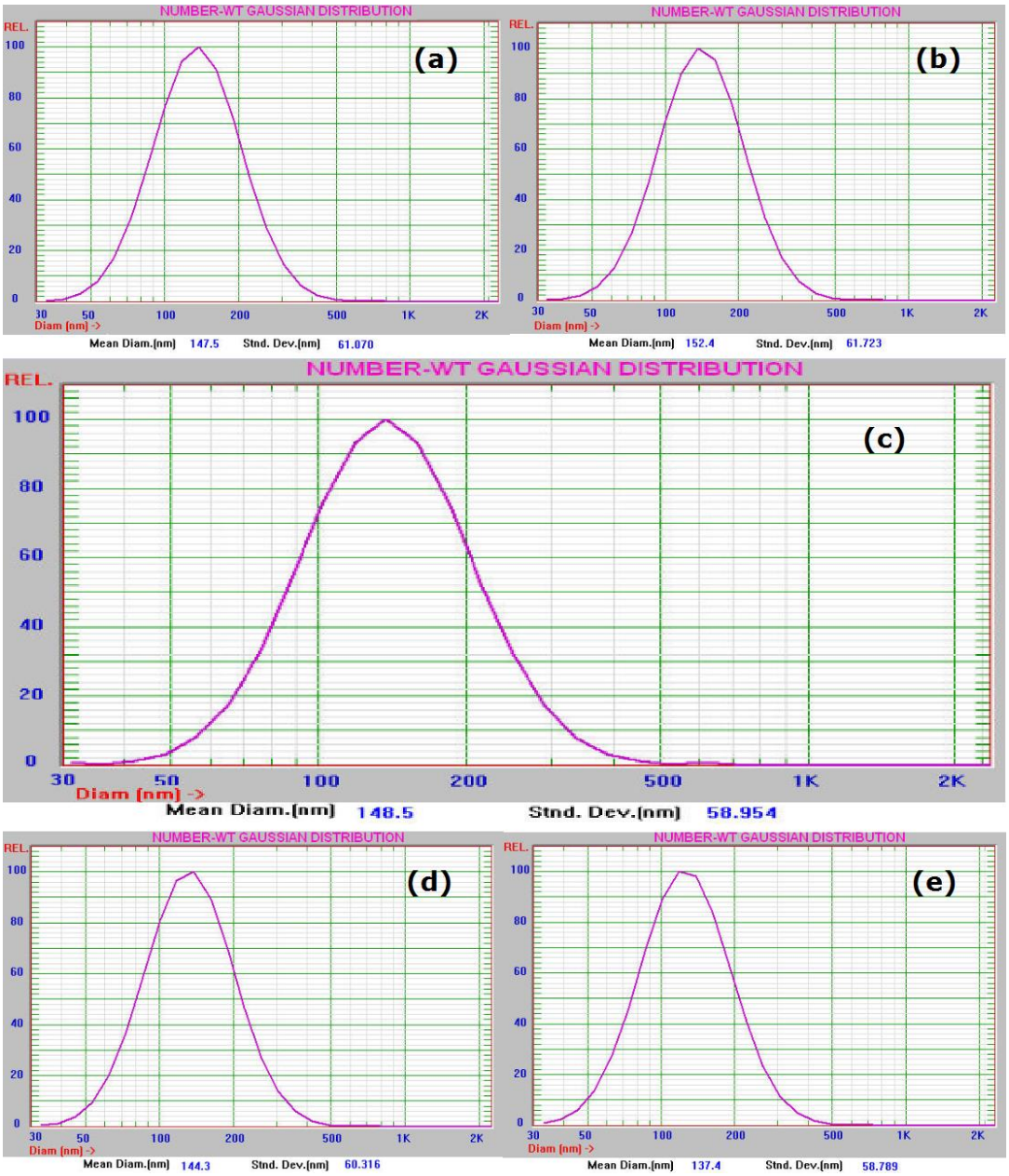

Figure 5 Number weighted particle size distributions for different alumina nanofluids at t = 0 sec, by NICOMP 380. At volume fraction 0.05 percent (a) pH = 3, C = 10^{-4}M (b) pH = 3.3, C = 10^{-3}M (c) pH = 4, C = 10^{-3}M (d) pH = 4, C = 10^{-4}M. At volume fraction 0.01 percent (e) pH = 4, C = 10^{-4}M. C is the concentration of NaCl measured in Molarity

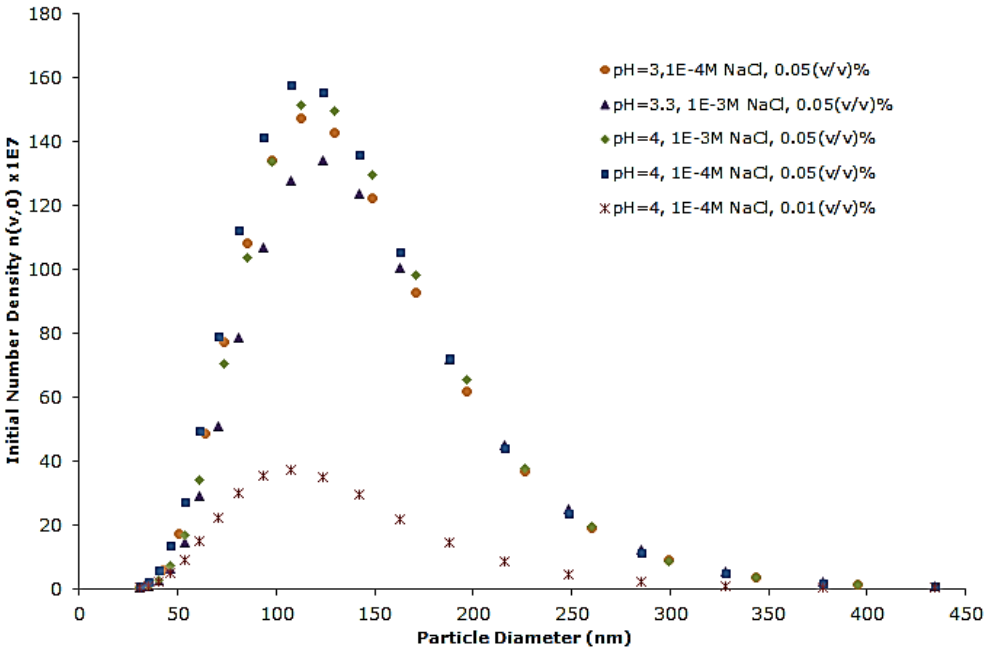

Figure 6 Initial particle number density distributions for alumina nanofluids, t = 0 sec

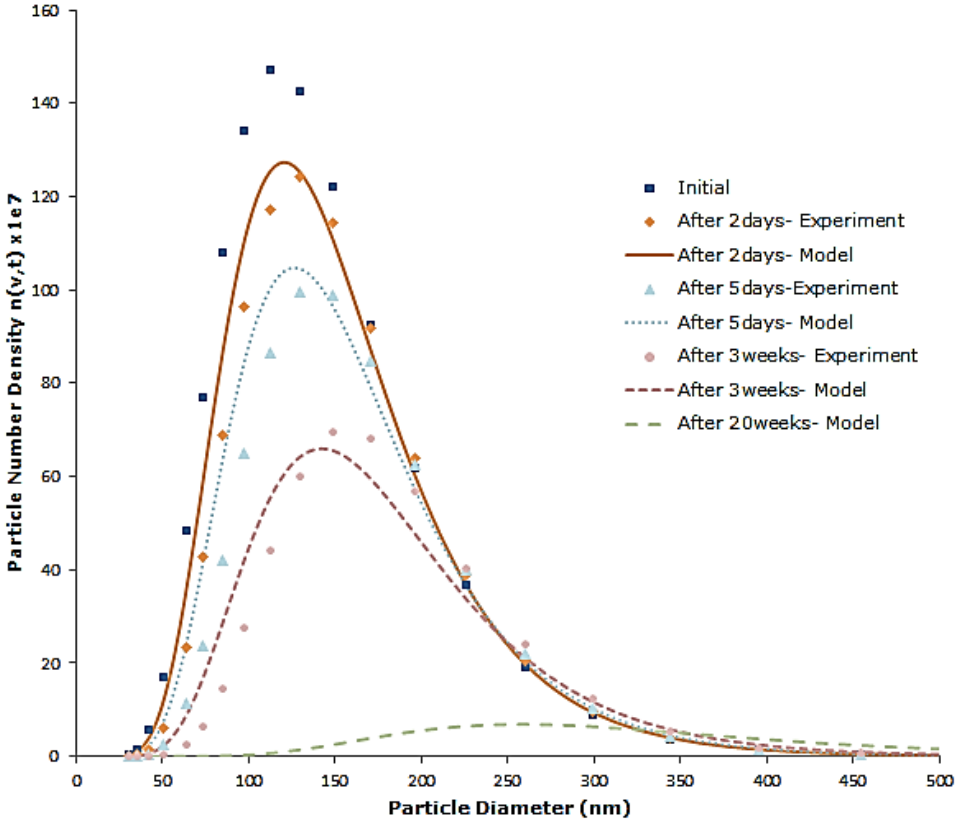

Figure 7 Particle number density distributions at different times for alumina nanofluid at 0.05 percent (v/v) with pH = 3 and 10^{-4}M of NaCl

With decrease in the pH from 4 to 3 the number of H^+ ions is increased 10 folds. These potential determining ions get adsorbed onto the surface of alumina nanoparticles creating a net charge on the surface. These charged particles are surrounded by the counter-ions, in this case Na^+ and Cl^-, forming a deybe layer of ions around the nanoparticles. With increase in the concentration of the counter-ions by increasing the electrolyte concentration the thickness of the debye layer decreased.

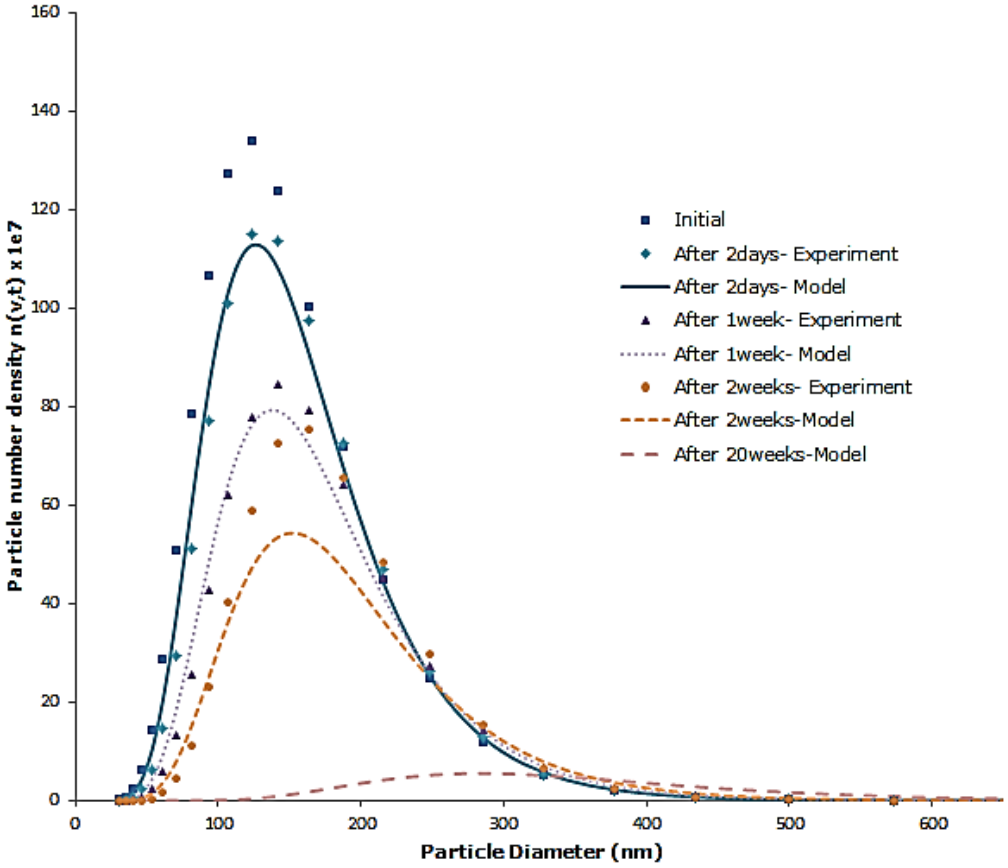

Figure 8 Particle number density distributions at different times for alumina nanofluid at 0.05 percent (v/v) with pH = 3.3 and 10^{-3}M of NaCl

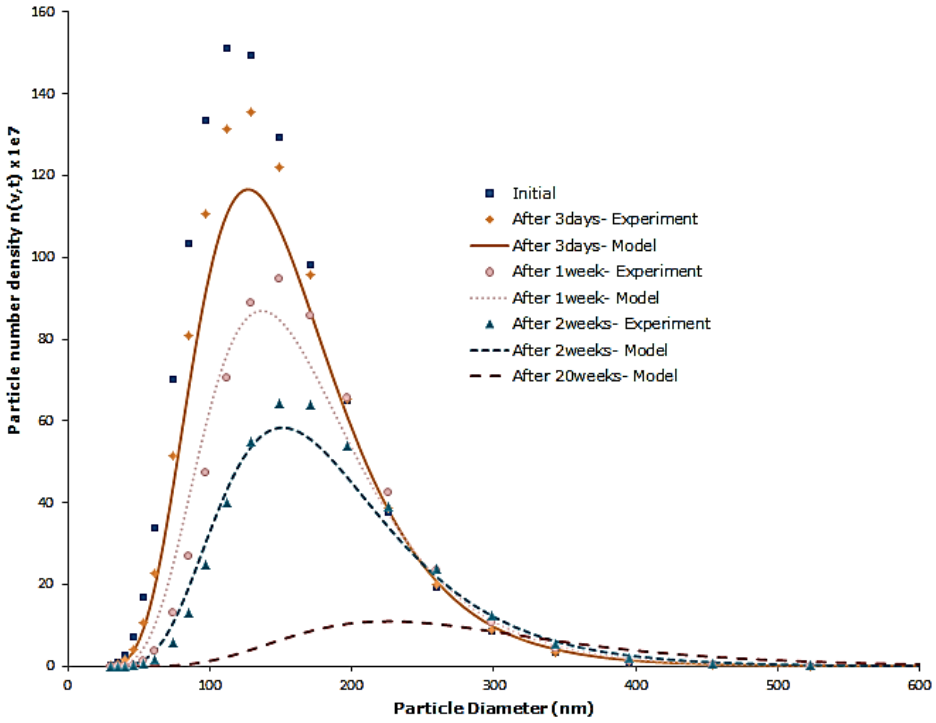

Figure 9 Particle number density distributions at different times for alumina nanofluid at 0.05 percent (v/v) with pH = 4.0 and 10^{-3}M of NaCl

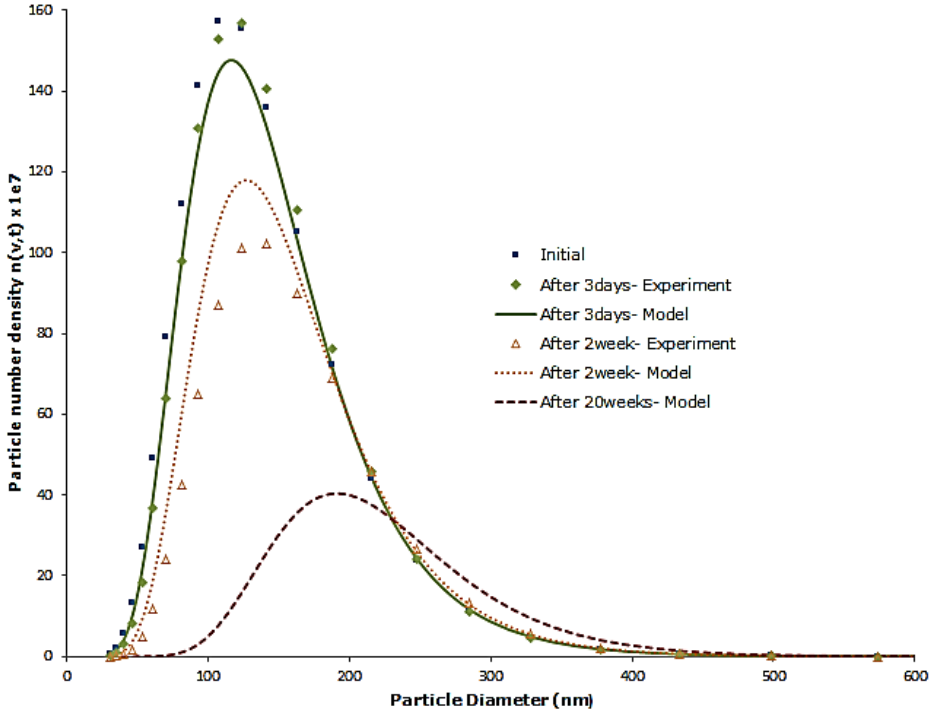

Figure 10 Particle number density distributions at different times for alumina nanofluid at 0.05 percent (v/v) with pH = 4.0 and 10^{-4}M of NaCl

The charge on the surface of nanoparticles is measured quantitatively by means of the zeta potential which measures the potential in the stern layer around the charged nanoparticle. At lower zeta potential vlaues, the stern potential (ψ) is assumed to be the same as the zeta potential. It has been observed by Wiese & Healy (1974) and Das et al. (2010) that the electrolyte concentration and the type of counter-ions could affect the zeta potential. By adding chloride ions to the alumina nanofluid, they get attached to the surface of the alumina particles decreasing the net charge on the particles thus decreasing the zeta potential considerably. Also with the increase in the electrolyte concentration the zeta potential can decrease due to increase in the specific ion concentration. As indicated in Figure 11, for alumina nanofluid at pH=4 and 5x10^{-4}M sodium chloride the zeta potential was as low as 20mV whereas it was about 40mV with same concentration of iodide and bromide ions. Taking these effects and uncertainty in the zeta potential measurements into consideration and assuming the zeta potential is constant throughout the life of nanofluid the expected extrapolated zeta potential of alumina nanofluids has been presented in Table 1.

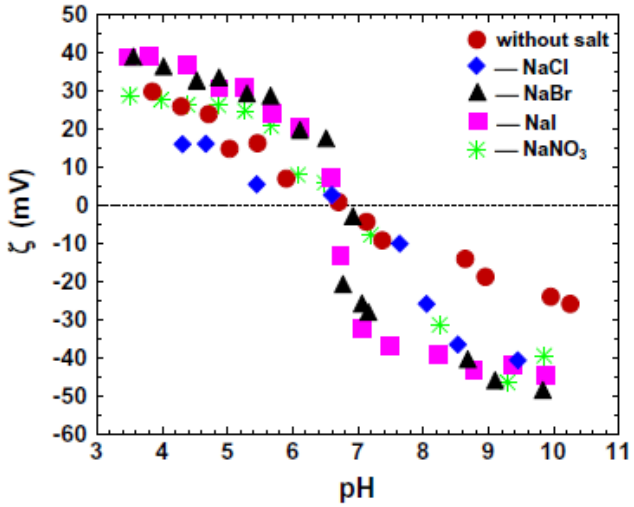

Figure 11 Variation of zeta potential of α- alumina nanofluid with pH in the presence of 5x10^{-4}M NaCl(aq.), NaBr(aq.) and $NaNO_3$(aq.) at 25°C. From Das et al. (2010)

Table 1 Parameters of alumina nanofluids at different pH and electrolyte concentration

Alumina Nanofluid	Total Ionic Concentration(M)	Zeta Potential(mV)	Debye Length(nm)
pH=3, 10^{-4}M NaCl	$1.2X10^{-3}$	35	12.6
pH=3.3, 10^{-3}M NaCl	$2.5X10^{-3}$	30	8.71
pH=4, 10^{-3}M NaCl	$2.1X10^{-3}$	28	9.50
pH=4, 10^{-4}M NaCl	$3.0X10^{-3}$	40	25.1

From Figure 6 and Table 1 it can be observed that the peak number density is lower for the alumina nanofluid with pH = 3.3 and 10^{-3}M NaCl which has lower zeta potential, and the peak number density is higher for the nanofluid with pH = 4 and 10^{-4}M NaCl which has higher zeta potential.

During agglomeration the smaller particles are prone to more number of collisions due to their higher diffusion coefficient, and form clusters of bigger particles. This can be observed in Figure 7 to 10 as the number of smaller particles is decreasing and number of bigger particles is increasing. Large decrease in the number of small particles account for a small increase in the number of bigger particles such that total volume of all the nanoparticles per unit volume of nanofluid remains constant with time.

Using the independent parameters as input for the numerical model viz., volume fraction, *pH*, electrolyte concentration, zeta potential, Hamaker constant and temperature of each nanofluid along with the initial average particle size and standard deviation of both the particle number and volume weighted distributions, the numerical model generated particle number distributions are compared with experimental results in Figure 7 to 10. The differences in the experimental and model distributions can be attributed to the assumptions in theoretical derivations of the expressions for interparticle potential energies, uncertainties in the measurement of zeta potential and experimental procedure, etc.

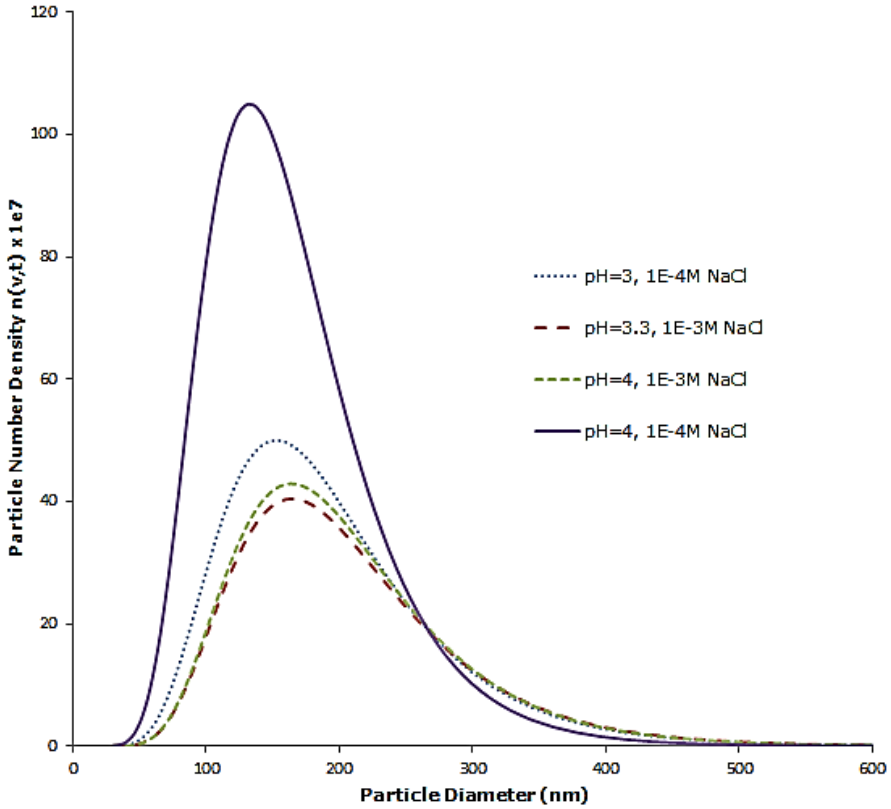

Figure 12 Particle number density distributions from model for different alumina nanofluids after 3 weeks

To understand the effect of pH and electrolyte concentration on agglomeration, particle number density distributions from model after 3 weeks for all alumina nanofluids are compared in Figure 12. Nanofluids with $pH =$ 3.3 and 10^{-3}M NaCl and $pH =$ 4 and 10^{-3}M NaCl having low zeta potential are observed to agglomerate at faster rate compared to others. But alumina nanofluid with $pH =$ 4 and 10^{-4}M NaCl is observed to have very slow rate of agglomeration compared to alumina nanofluid with $pH =$ 3 and 10^{-4}M NaCl although the zeta potential values have no much difference. This is due to decrease in the electrostatic double layer repulsion energy which includes effect of both the zeta potential and the counter-ion concentration. With increase in the counter-ion concentration the thickness of the electrical double layer decreased (Table 1) thus decreasing the repulsive forces between the particles (Figure 13). Among the alumina nanofluids prepared here, the nanofluid with higher zeta potential and lower

concentration (with $pH = 4$ and 10^{-4}M NaCl) is having less average particle size than the nanofluid with lower zeta potential and high counter-ion concentration (with $pH = 3.3$ and 10^{-3}M NaCl) at any time, thus indicating more shelf life period for alumina nanofluid with $pH = 4$ and 10^{-4}M NaCl compared to alumina nanofluid with $pH = 3.3$ and 10^{-3}M NaCl.

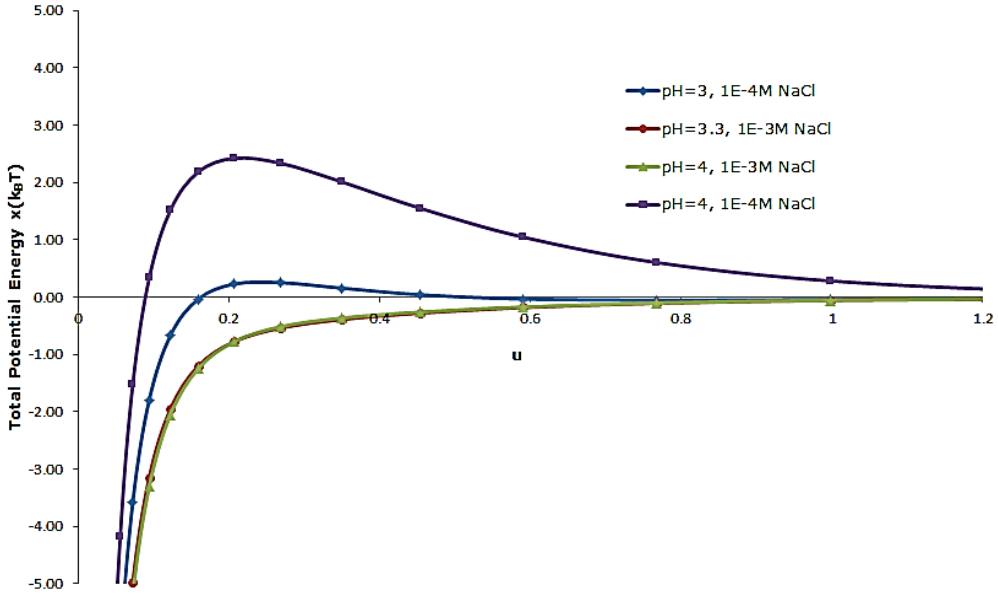

Figure 13 Total interaction energy between two particles each of dia. 150nm in alumina nanofluids. 'u' is scaled distance between the surfaces of particles

The average particle diameters for PSDs for alumina nanofluids with different properties and at different times can be used to quantitatively estimate the extent of agglomeration. Since the numerical model results are compared with a reasonable certainty with experimental results, average particle diameter values for PSDs of alumina nanofluids can be used either from experimental analysis or from numerical modeling(Table 2). The average particle size in alumina nanofluid - 3 (Table 2) with very low zeta potential (Table 1) was increased by 28 percent in 2 weeks, and in alumina nanofluid – 4 with high zeta potential (Table 1) it was increased by 14 percent in 2 weeks. This clearly shows that agglomeration is faster in alumina nanofluid – 3 compared to alumina nanofluid – 4. From the numerical model analysis it can be estimated that in 20 weeks the average particle size in alumina nanofluid - 3 will

increase by 133 percent, whereas the average particle size in alumina nanofluid – 4 will increase by only 54 percent. Large changes in the average particle size in nanofluids may cause inconsistencies in the performance during industrial applications. Alumina nanofluid – 3 with faster agglomeration than alumina nanofluid – 4 has shorter than 20 weeks of shelf life period thus cannot be used in industrial applications for longer duration.

Table 2 Average particle dia. (nm) and standard deviation (nm) for particle size distributions by experimental analysis and numerical modeling at different times for alumina nanofluids. C is the concentration of electrolyte in Molarity

Alumina Nanofluid	Properties	Time	Average Particle Diameter (nm)		Standard Deviation (nm)	
			Experiment	Model	Experiment	Model
1	0.05 percent (v/v), pH=3, C=10^{-4}M	0 sec	147.5	147.5	61.1	61.1
		2 days	157.7	152.9	61.3	63.5
		5 days	167.9	160.7	63.3	66.8
		3 weeks	187.6	194.0	66.8	80.6
2	0.05 percent (v/v), pH=3.3, C=10^{-3}M	0 sec	152.4	152.4	61.7	61.7
		2 days	160.8	158.9	61.9	64.5
		1 week	175.1	173.7	66.5	70.7
		2 weeks	185.7	191.4	64.4	77.8
3	0.05 percent (v/v), pH=4, C=10^{-3}M	0 sec	148.5	148.5	59.0	59.0
		3 days	154.0	158.7	59.9	63.4
		1 week	174.6	170.9	61.6	68.4
		2 weeks	190.4	189.1	68.5	75.7
4	0.05 percent (v/v), pH=4, C=10^{-4}M	0 sec	144.3	144.3	60.3	60.3
		3 days	147.2	147.5	58.6	60.9
		2 weeks	165.1	158.3	64.1	63.0

Having successfully comparing the results of numerical model with experimental results with alumina nanofluids, the PSDs of different nanofluids can be obtained for longer durations which help in estimating the shelf life of nanofluids.

Chapter 5. Conclusions and Future Scope

A numerical model has been created to understand and address the agglomeration effects on the shelf life of nanofluids. Starting with knowledge of independent variables like volume fraction, pH, electrolyte concentration and zeta potential, and Hamaker constant along with the initial particle size distribution (PSD), the model is able to predict the temporal changes in PSDs. Experimental measurements have been made using Alumina nanofluids to successfully validate the model and the results are presented here. The differences in the PSDs of nanofluids with different pH and electrolyte concentration are quantitatively explained based on Deryaguin, Landau, Verwey, and Overbeek (DLVO) theory. Alumina nanofluids with higher zeta potential and lower counter ion concentrations have longer shelf life period compared to the nanofluids with lower zeta potential and higher electrolyte concentration. The reasons for longer shelf life are attributable to changes in the electrostatic double layer interaction energy between the particles. From the numerical model analysis it can be estimated that in 20 weeks the average particle size in alumina nanofluid with pH = 4 and 10^{-3}M of NaCl will increase by 133 percent, whereas the average particle size in alumina nanofluid with pH = 4 and 10^{-4}M of NaCl will increase by only 54 percent. Alumina nanofluid with pH = 4 and 10^{-3}M of NaCl with faster agglomeration than alumina nanofluid pH = 4 and 10^{-4}M of NaCl has shorter than 20 weeks of shelf life period thus cannot be used in industrial applications for longer duration. With the model presented here, knowing the independent parameters, the shelf life period for any nanofluid can be estimated with reasonable certainty.

As a part of the future studies, this numerical model developed here can be extended to nanofluids having steric repulsions due to polymeric stabilizers, by including the effects of steric repulsions on the total interaction energy between the particles. This numerical model could be extended to different shapes of the nanoparticles and could be

compared by performing experimental analysis with different nanoparticles of different sizes and variety of electrolytes.

Bibliography

Choi, S. (1995). Enhancing thermal conductivity of fluids with nanoparticles. *In Developments and Applications of Non-Newtonian Flows, ed. DA Siginer, HP Wang*, 99-105.

Das, M. R., Borah, J. M., Kunz, W., Ninham, B. W., & Mahiuddin, S. (2010). Ion specificity of the zeta potential of alpha-alumina, and of the adsorption of p-hydroxybenzoate at the alphha-alumina–water interface. *Journal of Colloid and Interface Science*, 344:482-491.

Das, S. K., Putra, N., & Roetzel, W. (2003). Pool boiling characteristics of nano-fluids. *International Journal of Heat and Mass Transfer*, 46:851-862.

Eastman, J., Choi, S., Li, S., Yu, W., & Thompson, L. (2001). Anomalously increased effective thermal conductivities of ethylene glycol-based nanofluids containing copper nanoparticles. *Applied Physics Letters*, 78:718-720.

Hamaker, H. C. (1937). The London-- van der Waals Attraction Between Spherical Particles. *Physica IV*, 4:1058-1072.

Hunter, R. J., & White, L. R. (1987). *Foundations of Colloid Science.* Oxford Oxfordshire and New York: Clarendon Press.

Islam, A., Chowdhry, B., & Snowden, M. (1995). Heteroaggregation in colloidal dispersions. *Advances in Colloid and Interface Science*, 62:109-136.

Kumar, S., & Ramkrishna, D. (1996). On The Solution of Population Balance Equations By Discretization--II. A Moving Pivot Technique. *Chemical Engineering Science*, 51:1333-1342.

Lee, D., Kim, J.-W., & Kim, B. G. (2006). A New Parameter to Control Heat Transport in Nanofluids: Surface Charge State of the Particle in Suspension. *J. Phys. Chem. B*, 110:4323-4328.

Lee, J.-H., Hwang, K. S., Jang, S. P., Lee, B. H., Kim, J. H., Choi, S. U., et al. (2008). Effective viscosities and thermal conductivities of aqueous nanofluids containing low volume concentrations of Al2O3 nanoparticles. *International Journal of Heat and Mass Transfer*, 51:2651-2656.

Lee, S., Choi, S., Li, S., & Eastman, J. (1999). Measuring thermal conductivity of fluids containing oxide nanoparticles. *Journal of Heat Transfer*, 121:280-289.

Lo, C.-H., & Tsung, T.-T. (2005). Low-Than-Room Temperature Effect On The Stability of CuO Nanofluid. *Reviews on advanced materials science*, 10:64-68.

Park, Y. K., Tadd, E. H., Zubris, M., & Tannenbaum, R. (2005). Size-controlled synthesis of alumina nanoparticles from aluminum alkoxides. *Materials Research Bulletin*, 40:1506-1512.

Sader, J. E., Carnie, S. L., & Chan, D. Y. (1995). Accurate Analytic Formulas For The Double-Layer Interaction Between Spheres. *Journal of Colloid and Interface Science*, 171:46-54.

Scott, W. T. (1967). Analytic Studies of Cloud Droplet Coalescence I. *Journal of Atmospheric Sciences*, 25:54-65.

Timofeeva, E. V., Gavrilov, A. N., McCloskey, J. M., & Tolmachev, Y. V. (2007). Thermal conductivity and particle agglomeration in alumina nanofluids: Experiment and theory. *Physical Review E*, 76:061703/1 – 061703/16.

Wiese, G., & Healy, T. (1974). Coagulation and electrokinetic behavior of TiO2 and Al2O3 colloidal dispersions. *Journal of Colloid and Interface Science*, 51:427-433.

Yang, Y., Oztekin, A., Neti, S., & Mohapatra, S. (2012). Particle agglomeration and properties of nanofluids. *Journal of Nanoparticle Research*, 14:852/1–852/10.

Appendix

A. Numerical Model

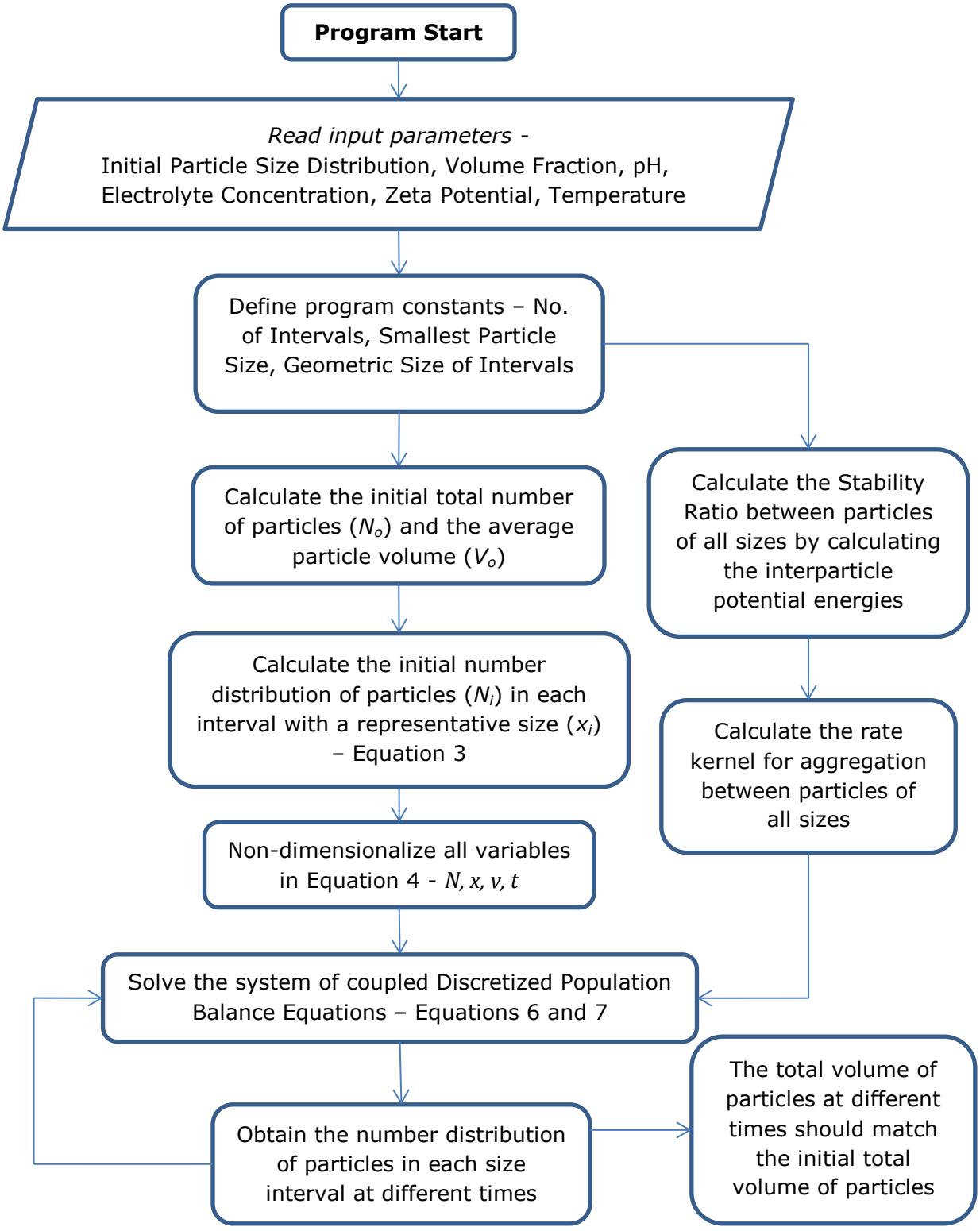

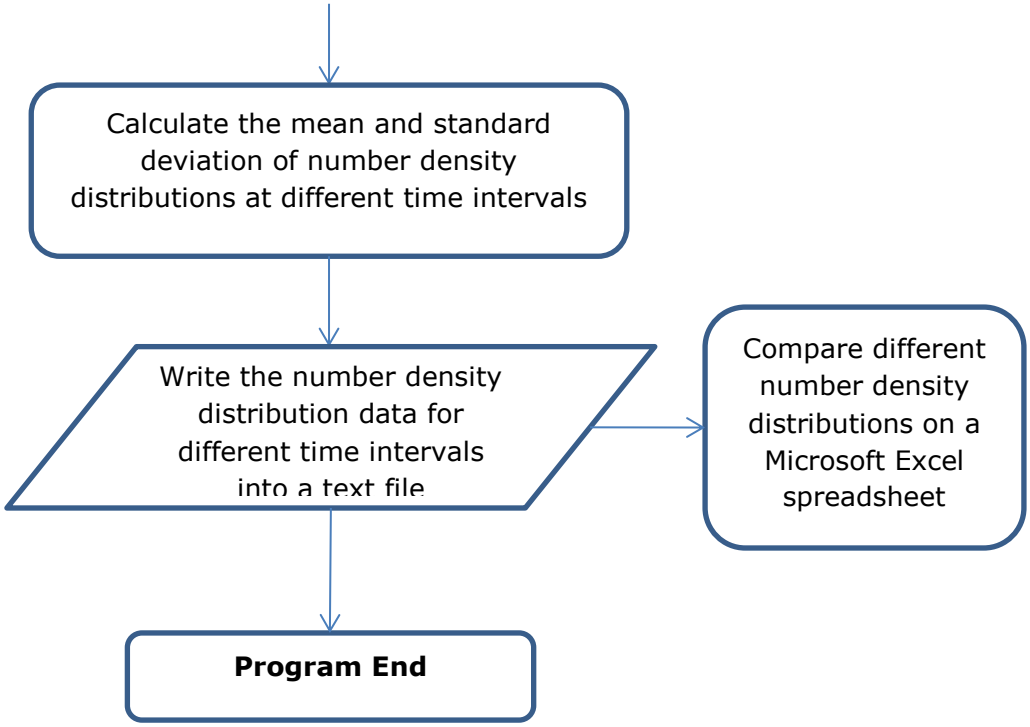
Calculate the mean and standard deviation of number density distributions at different time intervals
Write the number density distribution data for different time intervals into a text file
Compare different number density distributions on a Microsoft Excel spreadsheet
Program End

Vita

Hari Krishna Kanagala son of Sankaram Kanagala and Dayakshi Kanagala was born on June 1st 1987 near Mylavaram in Andhra Pradesh, India. All his education till intermediate level was completed in Andhra Pradesh. He pursued his Bachelor of Technology degree in Mechanical Engineering from Indian Institute of Technology Madras, India in 2009. He has published his undergraduate research work on Pool Boiling Characteristics of Metallic Nanofluids in the Journal of Heat Transfer in 2011 which has been cited 4 times till date. He started his professional career as a Project Engineer at Steel Authority of India Ltd and worked with that company between 2009 and 2011. At Present, he is submitting his thesis towards completion of his Master of Science degree at Lehigh University.